Methylbenzene Chemistry on Zeolite HBeta: Multiple Insights into Methanol-to-Olefin Catalysis

Alain Sassi, Mark A. Wildman, Hee Jung Ahn, Paritosh Prasad,† John B. Nicholas,‡ and James F. Haw*

Loker Hydrocarbon Research Institute and Department of Chemistry, University of Southern California, University Park, Los Angeles, California 90089-1661

Received: September 5, 2001; In Final Form: December 8, 2001

The reactions of 1,2,4-trimethylbenzene, 1,2,4,5-tetramethylbenzene (durene), pentamethylbenzene, hexamethylbenzene (HMB), ethylbenzene, and cumene were studied on large-pore zeolite HBeta catalysts, either alone or with co-injection of methanol-^{13}C. The reactivity of the methylbenzenes alone increased with increasing methyl substitution, as did selectivity for propene over ethylene. Disproportionation occurred for all methylbenzenes studied; in the case of HMB, pentamethylbenzene was a major volatile product, and we inferred that the heptamethylbenzenium cation also formed and remained in the catalyst. Substantially higher yields of olefins were obtained when methylbenzenes were co-reacted with methanol-^{13}C. Ethylbenzene alone was unreactive at 350 °C, but when injected with five equivalents of methanol-^{13}C, ethylbenzene formed ethylene-$^{12}C_2$ with very high selectivity. These and other experiments led to a detailed description of the hydrocarbon pool mechanism for MTO chemistry with side-chain methylation as the predominant route to olefins and the paring reaction as a possible minor pathway.

Introduction

The conversion of methanol to olefins or other hydrocarbons on solid acid catalysts has been intensely studied for a quarter century.[1−4] At least 20 distinct mechanisms were once considered for the formation of ethylene or other primary hydrocarbon products, but the reaction is now known to proceed through hydrocarbon-pool routes on the most important catalysts—zeolite HZSM-5[5−7] and the silico-aluminophosphate HSAPO-34.[8−12] The hydrocarbon-pool mechanism posits that carbon−carbon bond-forming and -breaking steps leading to olefinic products occur on larger hydrocarbon species (reaction centers) that work in concert with one or more acid sites and are regenerated in catalytic cycles. Organic reaction centers act as scaffolds that stabilize intermediates and transition states that would, on their own, be of prohibitively high energy.

The hydrocarbon pool species identified thus far include methylbenzenes, which function on both HSAPO-34 and HZSM-5, and cyclic carbenium ions, certainly the cyclopenentenyl cations such as **1** and also probably methylbenzenium cations such as **2**,[13] each of which can form on HZSM-5 during methanol conversion. Cation **1** is also an intermediate in the formation of toluene[6] and cation **2** can be synthesized in HZSM-5 by methylation of aromatics. Whatever the specific identity of the hydrocarbon pool species, they tend to form in the microporous solid acid catalyst by reactions of impurities in the methanol feed, and once in place the kinetic induction period for hydrocarbon synthesis from methanol (or dimethyl ether) ends.

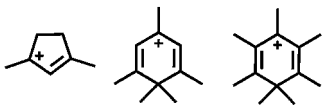

1 **2** **3**

Recently we combined GC analysis of olefin products and pulse-quench in situ NMR to correlate MTO product selectivity with the structure of the hydrocarbon pool species on HSAPO-34.[11] That study revealed that methylbenzenes trapped in the cages of HSAPO-34 could still eliminate ethylene and propene long after termination of methanol flow. The correlated results showed that methylbenzenes with five or six methyl groups per ring were most active for olefin formation and these formed propene with greater selectivity than for ethylene. Benzenes with fewer methyl groups were less active but showed higher ethylene selectivity with ethylene actually becoming predominant with three methyl groups per ring. Aromatics, even benzene, cannot pass through the eight-ring windows that interconnect the cages of HSAPO-34, but must be prepared in place by ship-in-a-bottle routes from olefins or other precursors. The ten-ring channels of zeolite HZSM-5 permit the entrance and egress of durene (1,2,4,5-tetramethylbenzene) but not penta- or hexamethylbenzene. Very recently, Arstad et al.[12b] showed, on the basis of isotopic scrambling studies on HSAPO-34, that polymethylbenzenes especially pentamethylbenzenes and hexamethylbenzenes are formed in the pores of the zeolite and play a key role in the MTO mechanism.

Thus, we looked to the 12-ring zeolite HBeta for an opportunity to directly introduce various methylbenzenes and other compounds for fundamental studies related to MTO chemistry. We studied the reactions of ethylbenzene, cumene, 1,2,4-trimethylbenzene, durene, pentamethylbenzene, and hexamethylbenzene (HMB) on HBeta. Both the rates of olefin

* Author to whom correspondence should be addressed.
† Present Address. Harvard Medical School, Cambridge, MA.
‡ Present Address. Genentech, Inc., 1 DNA Way, South San Francisco, CA 94065.

10.1021/jp013392k CCC: $22.00 © 2002 American Chemical Society
Published on Web 02/06/2002

elimination and propene selectivity increased with the number of methyl groups on the ring, and activity also increased greatly with increases in acid site density. Several fascinating observations bear on the detailed mechanism of MTO catalysis. Solutions of methanol and toluene (5:1 mol:mol) or methanol and trimethylbenzene (3:1 mol:mol) were far more active in the formation of olefins than either HMB alone or water and HMB (5:1 mol:mol). These results are interpreted to show that side-chain methylation competes with aromatic ring methylation, and the former more directly leads to the elimination of olefinic products. The volatile products exiting the reactor included trace (high ppm to low ppt) levels of various isopropyl-substituted methylbenzenes, and these were in reversible equilibrium with propene and methylbenzenes. Experiments using ethylbenzene and cumene reinforced the roles of alkyl side-chains in the MTO reaction mechanism.

When HMB alone was injected onto HBeta catalyst beds, the major product was pentamethylbenzene, and the amount formed was related to the ratio of reactant molecules to acid sites. We propose that HMB disproportionates on an acid site of HBeta to pentamethylbenzene and the heptamethylbenzenium cation **3**, the latter being trapped in the zeolite until liberated by a suitable reaction. Other observations support the idea that **3** deprotonates to form an exocyclic olefin necessary for side-chain methylation under acid catalysis. An alternative mechanism involving ring contraction and expansion (6 ⇄ 5) may operate at lower rates, especially in the absence of methanol, but it is clearly less important than side-chain methylation on zeolite HBeta.

Experimental Section

Materials and Reagents. Methanol-^{13}C (99%) was obtained from Cambridge Isotope Laboratories. Hexamethylbenzene (99+%) (HMB) was obtained from Acros Organics, while toluene (99.8%), pentamethylbenzene (99%), 1,2,4,5-tetramethylbenzene (98%) (durene), 1,2,4-trimethylbenzene (98%), ethylbenzene (99%), and cumene (99%) were purchased from Aldrich. Zeolyst International supplied the samples of zeolite HBeta (BEA). These were: CP814E (SiO_2/Al_2O_3 = 25), CP811E-75 (SiO_2/Al_2O_3 = 75), CP811E-150 (SiO_2/Al_2O_3 = 150), and CP811C-300 (SiO_2/Al_2O_3 = 300). Hexamethylbenzene-d_{18} was obtained from Cambridge Isotope Laboratories.

Catalysis. HMB has normal melting and boiling points of 168 °C and 264 °C, respectively. We developed the benchtop microreactor system in Figure 1 for experimentation with HMB as well as pentamethylbenzene or durene, which are also solids at room temperature. All metal components contacting the catalyst, reactants, or products were stainless steel. Solids were introduced using a heated chamber consisting of a heated tube 14 cm long by 0.65 cm i.d. isolated by two NUPRO model SS-6BG-3D pneumatically actuated valves. Typically we loaded 0.123 mmol of the solid methylbenzene into the chamber and then purged with He before closing the valve to isolate the reactant. In cases where it was necessary to also inject methanol or water coincident with HMB, we included a conventional pneumatically actuated liquid injection valve with the second reagent contained in a sample loop. The chamber and valves were wrapped with heating tape. Immediately prior to reactant injection, heating tape was used to rapidly heat the chamber and valves to 350 °C, and the vaporized hydrocarbon was introduced to the reactor by actuating valves to simultaneously open the chamber and close the bypass. If methanol or water were also to be introduced, the liquid sample valve would also fire as the chamber opened to the gas flow. He (600 sccm) was used as the carrier gas in all experiments.

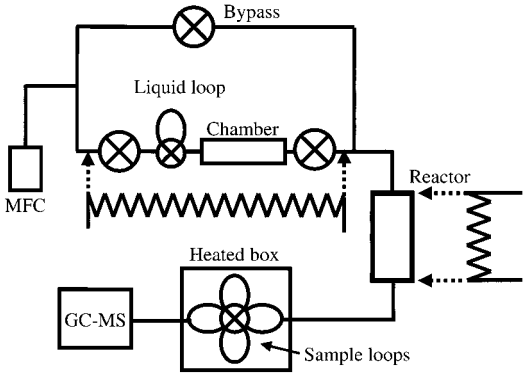

Figure 1. Diagram of the apparatus used to pulse HMB, pentamethylbenzene, or durene (all high-boiling solids) onto a zeolite HBeta catalyst bed and collect gas samples for GC-MS analysis. The stainless steel chamber tube (dimensions in Experimental Section) was loaded with solid hydrocarbon, placed in line, and purged with He. Immediately prior to injection heating tape was used to rapidly heat the chamber to 350 °C. The liquid loop was installed only when a second, liquid component (methanol-^{13}C or water) was to be co-injected. The apparatus was also used to inject liquids alone, in which case the chamber was removed. All lines between the sample chamber and the heated box were heated to minimize condensation. MFC denotes mass-flow controller.

The reactor (5 cm long, 0.65 cm i.d.) was loaded with 300 mg of fresh HBeta for each experiment, which was activated in place immediately prior to use by heating at 500 °C for 1 h in flowing helium. All tubing downstream of the chamber was heated. A Valco 16-position valve was used to collect up to eight gas samples. Since the first sample gathered (1.5 s after reagent injection) usually proved more informative than samples gathered at later times, we usually collected only two samples for GC-MS analysis, at 1.5 and 3.0 s. These samples were stored in 1 mL loops in a heated box (150 °C) while awaiting injection into the GC-MS.

Gas Chromatography−Mass Spectrometry. Reaction products were separated by gas chromatography (Agilent 6890 Series GC system) equipped with a capillary column Petrocol DH 150 (Fused Silica capillary column, 150 m long, 0.25 mm diameter, 1.0 μm film thickness). The temperature program maintained the oven temperature at 35 °C for an initial 25 min followed by a ramp of 20 °C/min to a final temperature of 290 °C. The products were analyzed by mass spectrometry (Agilent 5973 Mass selective detector) using an ionization voltage of 69.9 eV and a source temperature of 240 °C.

Results

Elimination of Olefins from Methylbenzenes Alone. Figure 2 presents GC-MS total ion chromatograms characterizing the volatile products from the reactions of methylbenzenes with three to six methyl groups on zeolite HBeta (SiO_2/Al_2O_3 = 75) at 450 °C. The yield of olefins from 1,2,4-trimethylbenzene (Figure 2a) was essentially zero, but this reactant isomerized to a mixture of all three trimethylbenzenes and also disproportionated to roughly equal amounts of xylenes and tetramethylbenzenes. Durene (Figure 2b) also isomerized and disproportionated to trimethylbenzenes and pentamethylbenzene (as well as smaller amounts of xylene and HMB), and it also gave traces of ethylene, propene, C_4 olefins, and propane and isoalkanes, the latter due to secondary reactions (vide infra). Pentamethylbenzene (Figure 2c) was severalfold more active than tetramethylbenzenes, and hexamethylbenzene (Figure 2d) was still more active, but even here the total conversion to olefins and alkanes was only ca. 2%.

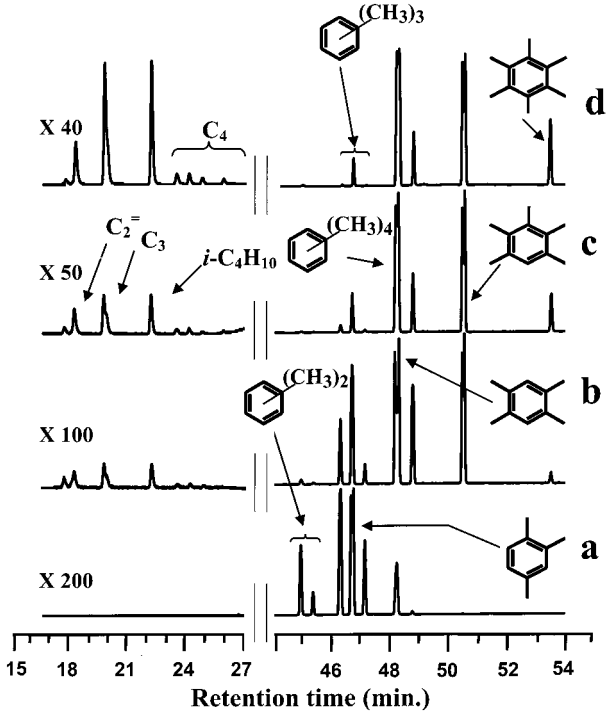

Figure 2. GC-MS total ion chromatograms from analyses of the volatile products exiting a catalytic reactor (300 mg zeolite HBeta, $SiO_2/Al_2O_3 = 75$, 450 °C) sampled 1.5 s following pulsed introduction of 0.123 mmol of various pure methylbenzene compounds. This loading corresponds to one molecule per acid site in the catalyst bed. Several of the more intense peaks in this and similar figures show structure due to overloading. The short retention time regions (olefins and light alkanes) are amplified as necessary for visualization of these products. (a) 1,2,4-Trimethylbenzene isomerizes and disproportionates but produces no detectable olefins on HBeta. (b) Durene (1,2,4,5-tetramethylbenzene) also isomerizes and disproportionates, and it eliminates 0.2% olefins with the highest ethylene selectivity in the Figure. (c) Pentamethylbenzene disproportionates and yields ca. 1% olefins and alkanes. (d) HMB eliminates a relatively higher yield of olefins, 2%, with the highest propene selectivity in the Figure. The large amounts of pentamethylbenzene and tetramethylbenzenes cannot be accounted for by olefin elimination alone.

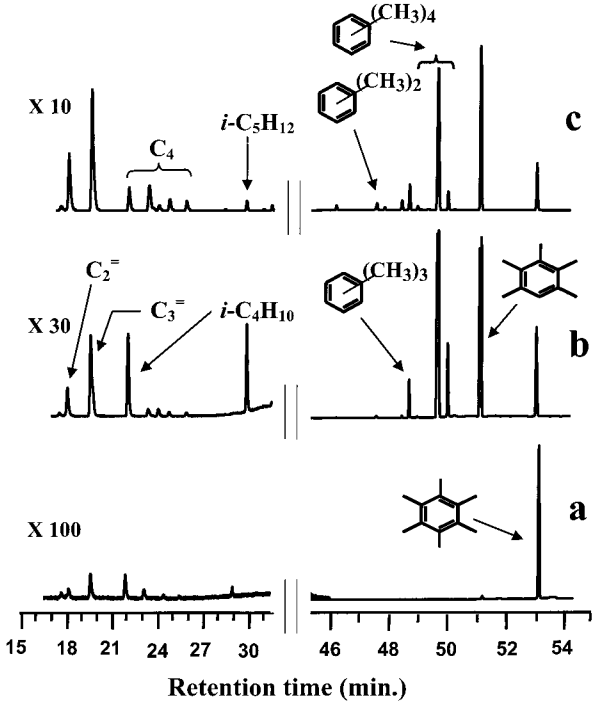

Figure 3. GC-MS total ion chromatograms from experiments probing the temperature dependence of the reactions of HMB (0.123 mmol) on 300 mg catalyst beds of HBeta ($SiO_2/Al_2O_3 = 75$). (a) At 350 °C HMB was almost completely unreactive. (b) It was modestly active for producing olefins at 450 °C. (c) At 550 °C conversion to olefins was greater than at 450 °C, ca. 37%. Alkane formation was suppressed at the higher temperature as well.

In Figure 2 the C_3 peak is in every case a mixture of propene and propane; the latter has a slightly longer retention time than the former and they can in any event be separately quantified by the mass spectra. The ratio of propene to ethylene is 1.1 for Figure 2b (tetramethylbenzene), 1.3 for Figure 2c (pentamethylbenzene), and 6.7 for Figure 2d (HMB). These numbers increase by a factor of 1.4 when the comparison is the ratio of total C_3 (propene and propane) to ethylene. In summary, Figure 2 shows that when methylbenzenes alone are pulsed onto a zeolite HBeta catalyst bed, the yield of olefins increases significantly as the number of methyl substituents increases, and so does the propene selectivity.

Figure 3 explores the temperature dependence of the reactivity of HMB on zeolite HBeta ($SiO_2/Al_2O_3 = 75$). The result at 450 °C (Figure 3b) has already been commented upon. The yield of olefins was negligible at 350 °C (Figure 3a), but the total yield of olefins and alkanes was ca. 37% at 550 °C (Figure 3c). We struck a balance between the need to see some reactivity for methylbenzenes alone (450 to 550 °C) and the desire to approximate the conditions used for methanol-to-olefin studies on HSAPO-34 and HZSM-5 (i.e., 350 to 400 °C) by operating at 450 °C for much of the work presented here.

Figure 4 compares the results of pulsing 20.0 mg of HMB onto catalyst beds of four different HBeta samples with varying SiO_2/Al_2O_3 ratios. In Figure 4a the SiO_2/Al_2O_3 ratio was 300 and there were four HMB molecules for every acid site. This experiment gave a remarkable result—the only significant product (in addition to HMB) was pentamethylbenzene. This counterintuitive finding is a major topic of the discussion section. Using the catalyst with a SiO_2/Al_2O_3 ratio of 150 (Figure 4b) for which there were two HMB molecules injected for every acid site, the products sampled at 1.5 s showed more pentamethylbenzene than HMB. Traces of olefinic products were also detected. Figure 4c shows the result from an analogous experiment on zeolite HBeta with a SiO_2/Al_2O_3 ratio of 75 (the HMB-to-acid site ratio was 1 to 1). Here there was not only pentamethylbenzene but also a significant amount of tetramethylbenzenes. The olefin and alkane yield again increased with the increase in acid site density, but only to ca. 2%. Olefin formation clearly does not account for the loss of one or two methyl groups from a majority of the aromatic molecules sampled at 1.5 s. The catalyst with a SiO_2/Al_2O_3 ratio of 25 (Figure 4d) was far more active for olefin and alkane formation, but even here the C_2 through C_5 yield was only ca. 26% of methylbenzene molecules eliminated an olefin. Figure 4d shows only a small amount of HMB; penta- and tetramethylbenzenes were the major aromatic products, and less highly substituted benzenes were also prominent.

Comparing the four GC-MS total ion chromatographs in Figure 4, one notes not only a trend in activity but also a trend in product selectivity. The catalyst with a SiO_2/Al_2O_3 ratio of 150 (Figure 4b) produces olefins, no detectable isopentane, and only the smallest trace of isobutane. These isoalkanes are significant products on the catalysts with higher SiO_2/Al_2O_3 ratios, and isobutane is the most important nonaromatic product on the catalyst with the highest site density. Also, a careful examination of the C_3 peak shows that whereas the yield of

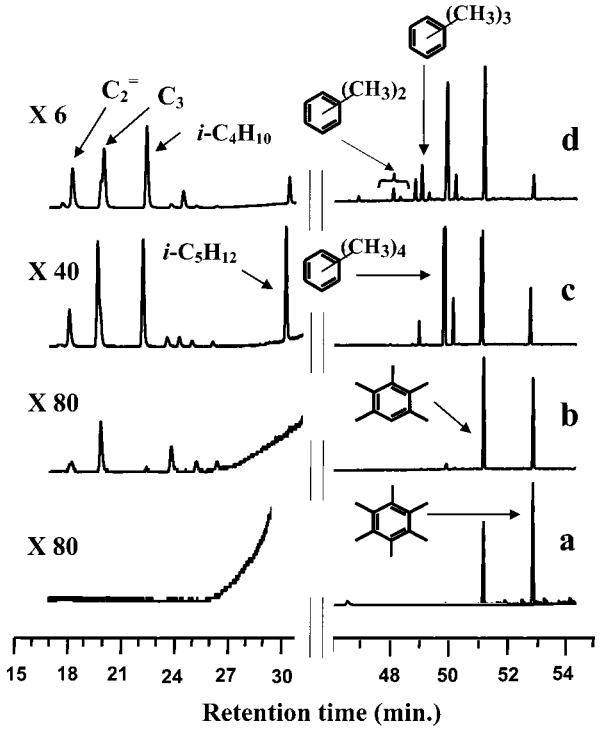

Figure 4. GC-MS total ion chromatograms from experiments probing the effect of varying the SiO_2/Al_2O_3 ratio of zeolite HBeta (300 mg per bed) on the conversion of HMB (0.123 mmol). The reactor temperature was 450 °C in each case. (a) On a catalyst with SiO_2/Al_2O_3 of 300 (four moles HMB per mole of acid sites) ca. 40% of the volatile product was pentamethylbenzene, but there were no detectable olefins. (b) On a catalyst with SiO_2/Al_2O_3 of 150 (two moles HMB per mole of acid sites) ca. 60% of the volatile product was pentamethylbenzene, and traces of olefins (ethylene, propene, and isobutene) were observed. (c) On a catalyst with SiO_2/Al_2O_3 of 75 (one mole HMB per mole of acid sites) the yield of olefins increased, but secondary reactions forming propane and isoalkanes were also significant. (d) On a catalyst with SiO_2/Al_2O_3 of 25 (one mole HMB per three moles of acid sites) decomposition of HMB to light products was greatly increased (ca. 26% yield of olefins and alkanes). On this zeolite with the highest acid site density studied, secondary reactions of olefins were so extensive that the propane yield exceeded that of propene.

propene exceeds that of propane on the zeolite with a SiO_2/Al_2O_3 ratio of 75, the order reverses on the catalyst with the highest acid site density. Alkane formation is characteristic of secondary reactions of olefins such as formation of cyclopentenyl carbenium ions and aromatics. The hydrogen lost in the formation of these cyclic products goes in part with the formation of propane and isoalkanes. Secondary reactions are more significant on catalysts with a high acid site density while an olefinic primary product is more likely to escape from a catalyst with fewer acid sites.

Reactions of Methylbenzenes with Methanol. The experiments reported in Figure 5 compare the reactions of (Figure 5a) HMB alone with those of either (Figure 5b) a 3 to 1 (mol:mol) solution of methanol and 1,2,4-trimethylbenzene, or (Figure 5c) a 5 to 1 (mol:mol) solution of methanol and toluene. These three experiments involved very similar reactants and they would be identical if aromatic ring methylation went to completion before any other reaction step and if the coproduct water is inconsequential. The control experiment in Figure 5d, water plus HMB (5 to 1 mol:mol), shows that water modestly altered the distribution of methylbenzenes exiting the reactor at 1.5 s, it did not increase the production of olefins, which was very low in both Figures 5a and 5d. Note that small amounts of methanol and dimethyl ether (DME) are seen in Figure 5d.

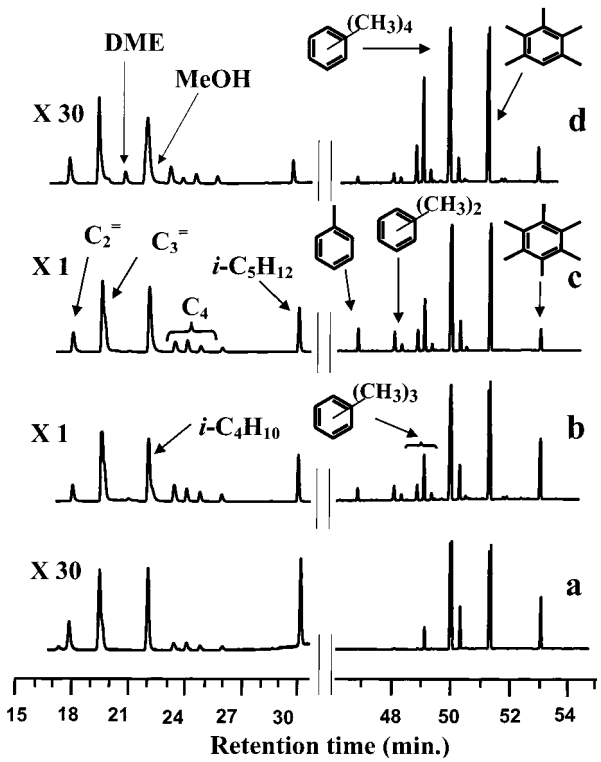

Figure 5. GC-MS total ion chromatograms from experiments probing the reactions of methylbenzenes with methanol-^{13}C. All experiments shown were carried out at 450 °C using HBeta with $SiO_2/Al_2O_3 = 75$ and gas sampling at 1.5 s. (a) HMB alone as a control. (a) Methanol-^{13}C and toluene 5:1 (mol:mol). (c) Methanol-^{13}C and 1,2,4-trimethylbenzene 3:1 (mol:mol). (d) Control experiment using water and HMB 5:1 (mol:mol). The solutions of methylbenzenes and methanol yielded far more olefins than the controls. Note that the overall stoichiometries of experiments (b) and (d) are similar and would be identical if the conversion of toluene and methanol to HMB and water went to completion before any other step.

Figures 5b and 5c show greatly enhanced conversion to olefins and alkanes. Clearly, some other reaction must have been occurring rapidly enough to compete with aromatic ring methylation, and this reaction lies on a pathway leading to olefinic products. A close examination of Figures 5b and 5c

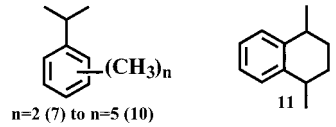

shows additional small peaks interspersed with those for the methylbenzenes that are not present in chromatograms of the unreacted aromatic starting materials. Some of these additional peaks are also present in the data depicted in Figure 5a (HMB alone), but at much lower levels than for reaction of trimethylbenzene or toluene with methanol. The chromatograms in Figure 6 are drawn so as to highlight and identify these peaks. Figure 6a is from the same experiment as Figure 5c, and Figures 6b and 6c are also from studies where 1,2,4-trimethylbenzene was reacted with three equivalents of methanol, but the catalysts used had lower acid site densities (Figure 6b, $SiO_2/Al_2O_3 = 150$; Figure 6c, $SiO_2/Al_2O_3 = 300$). Many of these species were present in all three of the results in Figure 6, although their levels varied with acid site density. *p*-Methylethylbenzene (**4**), cumene (**5**), and *p*-diethylbenzene (**6**) were identified unambiguously by injection of authentic samples. Many of the minority species had one isopropyl group and two (**7**), three (**8**), four

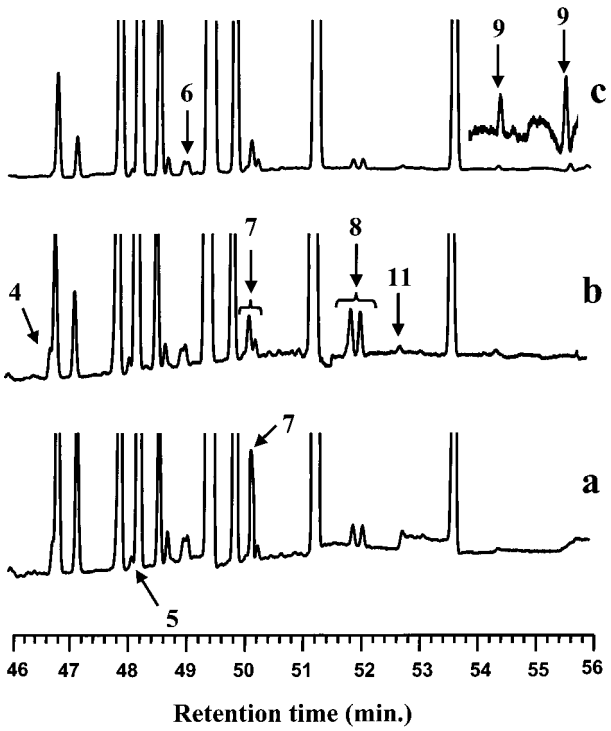

Figure 6. Expanded views of GC-MS total ion chromatograms from experiments in which methanol-^{13}C and 1,2,4-trimethylbenzene 3:1 (mol:mol) were pulsed onto various zeolite HBeta catalyst beds at 450 °C. These plots emphasize peaks due to various aromatic products (**4** through **10**, identified in the text), most of which have ethyl or isopropyl groups. (a) $SiO_2/Al_2O_3 = 75$. (b) $SiO_2/Al_2O_3 = 150$. (c) $SiO_2/Al_2O_3 = 300$.

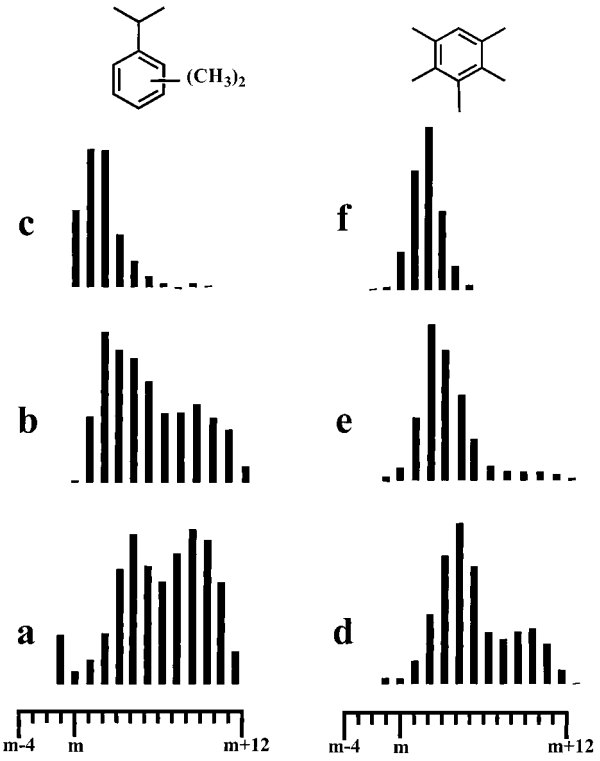

Figure 7. Bar graphs showing ion mass distributions in the vicinity of the molecular ions for isopropyldimethylbenzene **(7)** (a) through (c) and pentamethylbenzene (d) through (e) from the experiments in the previous Figure. (a) and (d) $SiO_2/Al_2O_3 = 75$. (b) and (e) $SiO_2/Al_2O_3 = 150$. (c) and (f) $SiO_2/Al_2O_3 = 300$. See the text for a detailed discussion of these distributions.

(**9**), or five (**10**) methyl groups. Species **7**, **8**, and **9** are identified in Figure 5; several are present as two or more isomers, but we are not able to assign specific substitution patterns on the basis of our mass spectra. **7** and isomers of methylcumene formed when we react 1,2,4-trimethylbenzene with one equivalent of 2-propanol (a propene source) under identical conditions (chromatogram not shown). Species **10** was identified in related experimental work using methanol and penta- or hexamethylbenzene (not shown). Species **11** is a tetralin derivative. The experimental mass spectrum was an exceptionally good match to that of **11** in the NIST database,[14] and it was a poor match to other possibilities in that collection. Thus, we assign it to the specific isomer shown. We speculate that **11** could form by coupling isopropyl groups ortho to each other.

The experiments in Figure 6, as well as closely related experiments, provided opportunities to probe the MTO reaction mechanism by following the fates of ^{13}C labels. Table 1 reports carbon isotope distributions for the ethylene and propene products from five such experiments. Propene had a higher ^{13}C content than ethylene. In every case, the fraction of ^{13}C in these olefins greatly exceeded that of the starting materials including all carbons (ring and methyl) of the aromatic co-feed. Furthermore, most of the results show that the ^{13}C content of ethylene and propene exceeded that of the methyl groups (methanols plus methyls on aromatics) in the starting materials.

The aromatic compounds exiting the reactor also showed varying degrees of carbon label scrambling, and the variation of exchange with structure as well as the detailed exchange distribution suggested mechanistic interpretations that we put forward in the Discussion section. Figure 7 reports bar graphs showing the ion mass distributions in the vicinities of the molecular ion peaks for pentamethylbenzene and one of the

TABLE 1: Carbon Label Distribution in Ethylene and Propene for Various Reactions

			ethylene				propene[c]				
system	% ^{13}C in starting material[a]	% $^{13}CH_3$ in starting material[b]	total ^{13}C in ethylene (%)	$^{13}C_0$ (%)	$^{13}C_1$ (%)	$^{13}C_2$ (%)	total ^{13}C in propene (%)	$^{13}C_0$ (%)	$^{13}C_1$ (%)	$^{13}C_2$ (%)	$^{13}C_3$ (%)
^{13}C-CH_3OH + toluene (5:1) on HBEA (75)	41.7	83.3	83.8	6.1	20.2	73.7	87.2	0.0	5.0	28.7	66.3
^{13}C-CH_3OH + 1,2,4-trimethylbenzene (3:1) on HBEA (75)	25.0	50.0	62.2	17.6	40.7	41.8	75.1	1.0	14.5	42.9	41.6
^{13}C-CH_3OH + 1,2,4-trimethlbenzene (3:1) on HBEA (150)	25.0	50.0	47.9	33.8	36.6	29.6	61.8	13.0	21.7	31.7	33.5
^{13}C-CH_3OH + 1,2,4-trimethylbenzene 3:1) on HBEA (300)	25.0	50.0	50.2	30.5	38.6	30.9	72.4	2.2	17.9	39.0	40.9
^{13}C-CH_3OH + hexamethylbenzene (5:1) on HBEA (75)	29.4	45.5	62.3	21.5	32.5	46.0	85.6	3.8	2.0	28.1	66.1

[a] Includes all carbons in both reactants. [b] Includes only methyl groups in both reactants and not ring carbons. [c] The yield of propene is in all cases several times that of ethylene.

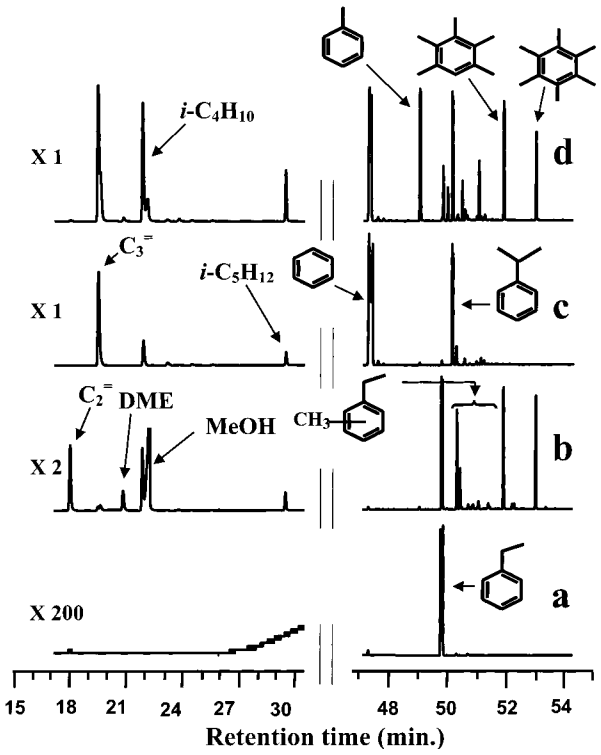

Figure 8. GC-MS total ion chromatograms from experiments probing the reactions of alkylbenzenes with methanol-^{13}C. All experiments shown were carried out at 350 °C using HBeta with $SiO_2/Al_2O_3 = 75$ and gas sampling at 1.5 s. All experiments used 0.123 mmol of alkylbenzene. (a) Ethylbenzene alone as a control. There was essentially no reaction on the catalyst. (b) Methanol-^{13}C and ethylbenzene 5:1 (mol:mol). There was a dramatic increase in ethylene yield. (c) Cumene alone as a control. This alkylbenzene was more reactive and formed moderate amounts of propene and secondary products of propene such as alkanes. (d) Methanol-^{13}C and cumene 5:1 (mol:mol). Note that the total yield of propene and C_3 to C_5 secondary products clearly exceeds that for cumene alone.

isopropyldimethylbenzene (**7**) isomers; these results are from the experiments in Figure 6. Note that **7** generally shows a higher degree of ^{13}C incorporation than pentamethylbenzene; in some cases, **7** has 10 or more ^{13}C labels, and this requires exchange into ring positions. Pentamethylbenzene shows a bimodal distribution of carbon isotopes. On the catalyst with a SiO_2/Al_2O_3 of 75 the larger population of pentamethylbenzene has zero to five ^{13}C labels, indicative of methyl exchange, while a smaller population has six to eleven ^{13}C labels. The latter result is consistent with synthesis of a methylbenzene from heavily ^{13}C-labeled olefins. Carbon label scrambling into ring positions was less evident for both aromatic products on the catalyst with the lowest acid site density.

Reactions of Ethylbenzene or Cumene with Methanol. Figure 8a shows that ethylbenzene (alone) is almost completely unreactive on HBeta at 350 °C. In sharp contrast, when the same charge of ethylbenzene was introduced with five equivalents of methanol-^{13}C (Figure 8b), there was a very high yield of ethylene, and this product contained almost exclusively ^{12}C (Table 2). The ethylene/propene ratio was 18, and this trace of propene had a high ^{13}C enrichment. The aromatic products in Figure 8b include unreacted ethylbenzene, isomers of ethylmethylbenzene, smaller amounts of ethyldimethylbenzenes, pentamethylbenzene, and HMB.

When cumene was pulsed onto HBeta at 350 °C much of it did eliminate propene (Figure 8c), but an ever greater yield was obtained when cumene was pulsed with five equivalents of methanol-^{13}C (Figure 8d). Not only was the propene yield higher in Figure 8d compared to 8c, the secondary reaction products of propene, especially propane, isobutane, and isopentane, were quite a bit higher as well. Thus, although it is clearly easier to eliminate an isopropyl group than an ethyl group, methylation of the ring is still helpful. Notable among the aromatic products in Figure 8d are low levels of two isomers of diisopropylbenzene, and even smaller amounts of species such as **7**.

H/D Exchange of HMB on HBeta at 450 °C. Using the device in Figure 1 we pulsed a charge of HMB onto HBeta (SiO_2/Al_2O_3 ratio of 75) exactly as in Figure 2d, except that here the HMB was 50% natural abundance and 50% HMB-d_{18}. GC-MS analysis of the product stream sampled at 1.5 s showed that the volatile products had somewhat greater than 50% H. The mass spectra of methylbenzenes exiting the catalyst bed showed clear evidence of exchange, and those results are presented in Figure 9. HMB and HMB-d_{18} had distinct retention times, and were chromatographically resolved almost to the baseline. The mass spectral patterns in this figure are the averages across entire GC peaks (or pairs of peaks) to accurately reflect the overall mass distributions.

HMB/HMB-d_{18} showed less extensive exchange that either pentamethylbenzene or durene, suggesting that much of the HMB observed at 1.5 s had a more limited contact with the catalyst. In Figure 9 we see near-mirror image patterns between mass m and mass $m + 18$. The peaks near or slightly above mass m are increased by loss of a methyl group from heavily deuterated HMB; for example, HMB-d_{18} (mass 180) loses CD_3 to contribute to the peak at 162, which is the mass peak for HMB. One sees this more clearly for loss of methyl from protonated HMB (i.e., m-15). Despite the complicating effect due to the difference of mass between HMB and HMB-d_{18} being identical to the mass of CD_3, the Figure clearly shows some degree of H/D exchange for HMB and HMB-d_{18}, and this exchange occurred one hydrogen at a time.

H/D exchange was more extensive and more easily interpreted for pentamethylbenzene and durene (Figure 9), for which the mass differences between the fully protonated and fully deuterated isomers are less than the mass of CD_3. Here we see very clearly that H/D exchange occurred one unit at a time and

TABLE 2: Carbon Label Distribution in Ethylene and Propene for Reactions of Ethylbenzene or Cumene with Labeled Methanol

	ethylene				propene				
system	total ^{13}C in ethylene (%)	$^{13}C_0$ (%)	$^{13}C_1$ (%)	$^{13}C_2$ (%)	total ^{13}C in propene (%)	$^{13}C_0$ (%)	$^{13}C_1$ (%)	$^{13}C_2$ (%)	$^{13}C_3$ (%)
^{13}C-CH_3OH + ethylbenzene (5:1) on HBEA (75)[a]	6.3	90.0	7.5	2.5	49.7	21.5	26.7	32.9	18.9
^{13}C-CH_3OH + cumene (5:1) on HBEA (75)[b]	43.4	33.6	46.0	20.4	14.3	74.2	12.8	9.2	3.9

[a] The yield of ethylene vastly exceeded that of propene. [b] The yield of propene vastly exceeded that of ethylene.

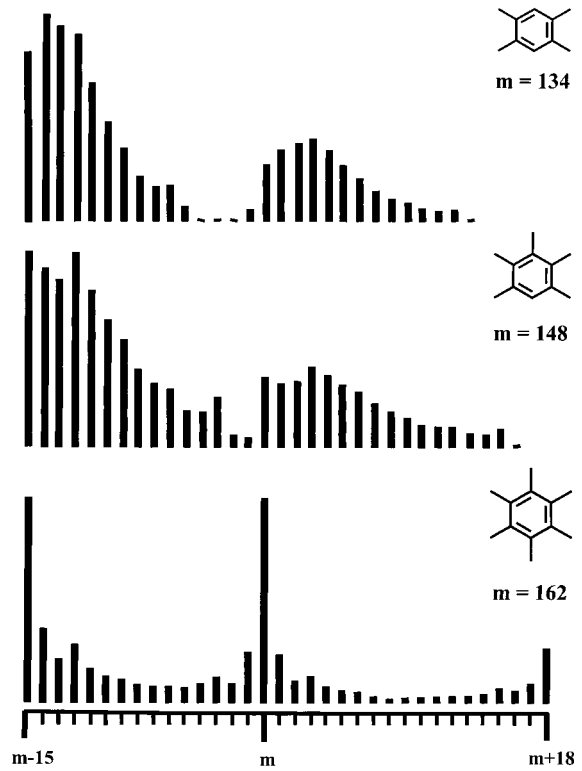

Figure 9. Bar graphs showing ion mass distributions in the vicinity of the molecular ions from GC-MS analyses of the volatile products exiting a catalytic reactor (300 mg zeolite HBeta, $SiO_2/Al_2O_3 = 75$, 450 °C) 1.5 s following pulsed introduction of 0.62 mmol of HMB and 0.62 mmol HMB-d_{18}. The reactions leading to durene and pentamethylbenzene included extensive H/D exchange that occurred in steps of one.

SCHEME 1

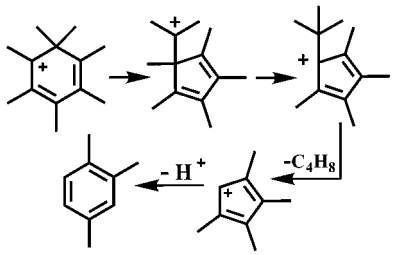

not simply three units at a time. This result does not of course preclude methyl exchange, and methyl exchange no doubt occurred in addition to a second exchange process.

Discussion

This Work in the Context of Several Previous Investigations. The experimental work presented above provides several clues that permit us to develop a detailed proposal for the structure and operation of the hydrocarbon pool on the 12-ring zeolite HBeta. In developing this proposal we are indebted to other contributions spanning a 40-year period. In particular, we acknowledge the 1961 paper by Sullivan and co-workers[15] on the "paring reaction" by which HMB hydrocracked on a bifunctional catalyst, liberating isobutane and other isoalkanes. Scheme 1 is a severely condensed version of the paring reaction described by Sullivan et al. As originally formulated, this mechanism began with protonation of HMB by an acid site of the bifunctional catalyst used in that work. We prefer methylation to protonation because of the evidence for *gem*-dimethylbenzenium cations (**2** and **3**) in acidic zeolites. Note that

SCHEME 2

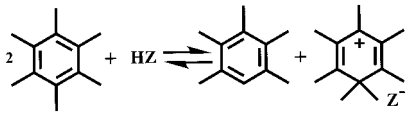

SCHEME 3

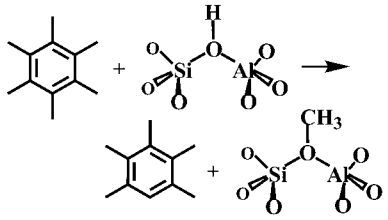

Scheme 1 (and especially its more detailed depiction in the original reference) permits the possibility of carbon label scrambling between ring and side-chain positions.

Another body of work that is highly relevant to this study is the early 1980s contributions of Mole et al. on the cocatalytic effect of toluene on methanol conversion on zeolite HZSM-5.[16,17] That work proposed the formation of benzenium cations (by protonaton), equilibration with exocyclic olefins, and side-chain methylation. We present an elaboration of this idea below. Chang's 1999 review of the mechanism of methanol conversion catalysis places much of this early work in the context of an emerging understanding of what is now called the hydrocarbon pool mechanism.[4] Kolboe coined the latter term,[8,9] and we used solid-state NMR, theoretical calculations, and isotope tracer methods to identify the species that function as the reaction centers on various catalysts.[5,6,10,11]

Methanol-to-Olefins (MTO) Reaction Mechanism. These observations reported here are consistent with the following mechanistic proposal: Disproportionation of *n*-methylbenzene into ($n + 1$)-methylbenzene and ($n - 1$)-methylbenzene is a general reaction on zeolite HBeta. For the case of $n = 6$ (HMB) disproportionation is still possible if we consume an acid site from the zeolite (HZ) and form the well-characterized heptamethylbenzenium cation **3** (Scheme 2).

This reaction was proposed in Sullivan's paper,[15] also to explain the observation of a surprising yield of pentamethylbenzene during the paring reaction of HMB on a bifunctional catalyst. In situ NMR and theoretical chemistry have established that the pentamethylbenzenium cation **2** is indefinitely persistent in zeolite HZSM-5 at room temperature,[13] and we recently established the persistence of the heptamethylbenzenium cation **3** in the more spacious HBeta using similar methods.[18] Those cations were synthesized in the zeolites for solid-state NMR investigation using benzene-$^{13}C_6$ and excesses of methanol.

The heptamethylbenzenium cation must remain in the vicinity of the zeolite framework anion site Z^-, while the pentamethylbenzenium cation is free to diffuse out of the HBeta catalyst bed and into the product stream. For completeness we also consider the reaction in Scheme 3 in which HMB reacts with HZ, now shown more explicitly, to form pentamethylbenzene and a framework-bound methoxy (methoxonium) group. We have found no evidence to suggest that the reaction in Scheme 3 contributes to our results, whereas formation of heptamethylbenzenium explains the very slow release of HMB from the catalyst, accounts for other features of olefin synthesis, and is supported by spectroscopic evidence.

There is no doubt that such methoxonium groups can form in other reactions on either basic aluminosilicate zeolites such as CsX[19] or on less strongly acidic solid acids such as HSAPO-

SCHEME 4

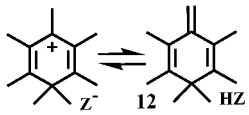

SCHEME 5

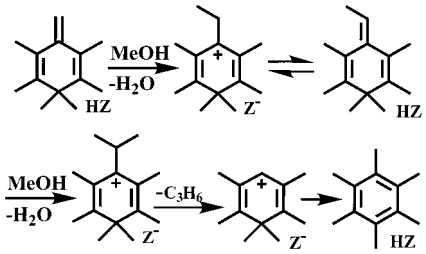

34,[10] but the evidence is mixed for the stability of methoxonium on more acidic zeolites such as HZSM-5 and HBeta. This methoxonium species was long considered an intermediate in toluene disproportionation, but a detailed investigation by Chang and co-workers concluded otherwise.[20] Either Scheme 2 or 3 could explain the observation in Figure 5d of small amounts of methanol and DME when HMB and water are co-injected.

Benzenium cations are only slightly less acidic than aluminosilicate zeolites. Scheme 4 shows the deprotonation of heptamethylbenzenium on the zeolite to form olefin **12** with its double bond necessarily exocyclic. Two of us recently calculated (MP4 single-point energies on MP2 geometries) the gas-phase proton affinity of the exocyclic olefin formed by deprotonation of benzenium cation **2**.[21] This value was 227.4 kcal/mol, and while we did not repeat these calculations for the heptamethyl cation **3**, we expect the value to be little changed by addition of methyl groups to the 3 and 5 positions. We also discovered that the threshold basicity for an olefin to be protonated on zeolite HZSM-5 was ca. 209 kcal/mol.[21] We would expect a complex of olefin **12** and the acid site HZ to be stabilized to an extent that equilibration of **3** and **12** occurs on the zeolite. There is long-standing evidence for Scheme 4 in acidic solution chemistry. In 1958 Doering and co-workers reported that they isolated exocyclic olefin **12** by pentane extraction of aqueous solutions of cation **3**.[22] Thus, if the acid strength is neither too low nor too high, species **3** and **12** will be in equilibrium, and this would provide facile H/D exchange, exactly as we observed for a mixture of HMB and HMB-d_{18} on HBeta.

Side-chain alkylation of toluene with methanol is usually regarded as being characteristic of a solid base catalyst such as CsX,[23] but an exocyclic olefin such as **12** creates the possibility of side-chain alkylation under acidic conditions. Mole and co-workers considered protonated rather than *gem*-dimethylated benzenium cations as well as starting materials with fewer methyl substituents;[16,17] however, their essential mechanism largely anticipated our proposal in Scheme 5 which shows formation of propene, the predominant primary product in our work.

One line of evidence supporting side-chain alkylation is the ^{13}C excess in ethylene and propene from experiments in which methanol-^{13}C reacted with unlabeled methylbenzenes (Table 1). If olefin synthesis occurred exclusively through a paring-type mechanism (i.e., ring methylation followed by ring contraction−expansion)[15] the ^{13}C content of the olefin products would be *lower* than that of methyls in the starting material due to the necessary incorporation of (unlabeled) ring carbons into the products. Alternatively, if methyl exchange between methanol and methyl positions on rings was more rapid than olefin

SCHEME 6

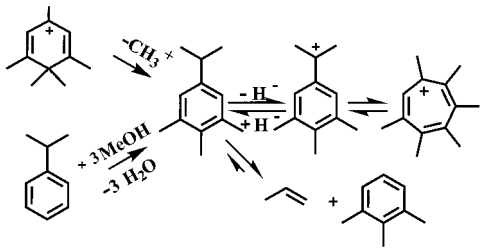

synthesis (and the paring rate was negligible) the carbon isotope distribution of the olefins would be identical to that of the starting methyl composition. Table 1 shows that for ethylene the ^{13}C incorporation is on average about equal to that of the methyl groups (methanol plus methyls on ring), while propene invariably had a higher ^{13}C enrichment. These results are not consistent with a paring mechanism. While Table 1 does support some degree of label scrambling prior to olefin synthesis, the higher ^{13}C content in propene argues for a chain growth mechanism with methanol-^{13}C providing the last carbon added to the chain.

The penultimate step in Scheme 5, elimination of propene with hydrogen transfer back to the ring, was shown to take place in a single transition state in a recent theoretical study of a similar reaction on a closely related cyclopentenyl carbenium ion.[6] We assume a similar step is possible here, although the same result could also be reached through more familiar detailed reaction steps. To complete a catalytic cycle a benzenium cation is regenerated in the zeolite by reaction of HMB or another methylbenzene with methanol. We earlier used this reaction to prepare cation **2** in HZSM-5 and cation **3** in HBeta from benzene-$^{13}C_6$ and methanol.[13,18]

Scheme 6 suggests how one of the intermediates in Scheme 5 can demethylate to form one of the isopropyl-substituted methylbenzenes that we observed in the product stream. We showed in Figure 8 that neutral hydrocarbons such as this can also form from the reaction of methanol with cumene, and that it may also eliminate propene. Finally, these compounds also form by back-reaction of products, as we demonstrated by introducing 2-propanol (a propene source) and trimethylbenzene (also shown in the scheme). Ring scrambling is assumed to occur when one of these isopropyl-substituted aromatics undergoes hydride abstraction, forming a stabilized tertiary benzyl cation. This opens the pathway to a tropylium cation,[24] and ring carbon scrambling then occurs through a 6 ⇆ 7 ring expansion−contraction route. The hydride abstraction in Scheme 6 requires (formally) a protonated olefin to act as an acceptor, leading to an alkane as a coproduct. This in turn requires a reasonable rate of olefin synthesis and conditions promoting secondary reactions leading to alkanes. Thus, in Figure 7 we see very extensive ring label scrambling in isopropyldimethylbenzene **7** on the catalyst with a SiO_2/Al_2O_3 ratio of 75 (Figure 7a), and a somewhat reduced degree of ring carbon scrambling on the catalyst with a SiO_2/Al_2O_3 ratio of 150 (Figure 7b). On the catalyst with a SiO_2/Al_2O_3 ratio of 300 (Figure 7c), most molecules of **7** have only two to five ^{13}C labels, as would be expected for side-chain scrambling with no ring scrambling. We have little olefin synthesis on this catalyst, which has the lowest acid site density of any we studied; hence there are few species to act as hydride acceptors. The ion mass distributions in Figure 7 are thus consistent with the proposed ring scrambling mechanism in Scheme 6.

Figure 7 also presents mass spectral ion distributions for pentamethylbenzene from those same experiments used to probe

SCHEME 7

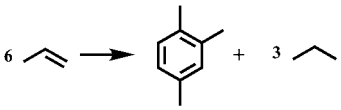

exchange for **7**. Secondary reactions also account for some of the features observed for this representative methylbenzene. Note the distinctly bimodal distribution for pentamethylbenzene formed by the reactions of trimethylbenzene and three equivalents of methanol-^{13}C on the catalyst with a SiO_2/Al_2O_3 ratio of 75 (Figure 7d). This distribution reveals that one population of pentamethylbenzene molecules undergoes only partial methyl exchange, resulting in mass peaks up to $m + 5$. A second population has a much higher ^{13}C content distribution. This bimodal distribution is apparent for the other methylbenzenes as well and it is reproducible. On the catalysts with the higher acid site densities, some of the olefin products will oligomerize, perhaps initially to methylcyclohexanes, and then rapidly form methylbenzenes, loosing hydrogen to other olefin molecules. Scheme 7 is one such balanced chemical reaction in which propene forms trimethylbenzene and three equivalents of propane for hydrogen mass balance. Since the propene formed in this experiment was highly enriched in ^{13}C (75% to be precise, Table 1), those methylbenzenes formed in reactions similar to that in Scheme 6 would have similar ring carbon enrichments. Thus, the existence of two populations in the ion-mass distribution of Figure 7d reflects both pentamethylbenzenes originally formed by methylation of trimethylbenzene—the lower mass population, and pentamethylbenzenes synthesized by secondary reactions similar to Scheme 6 followed by additional methylation or disproportionation—the higher mass population. Secondary reactions leading to labeled pentamethylbenzene are greatly reduced on the catalyst with a SiO_2/Al_2O_3 ratio of 150 (Figure 7e). The results for pentamethylbenzene on the catalyst with the lowest acid site density (Figure 7f) are consistent with no secondary synthesis from labeled propene, only methyl exchange need be invoked.

Olefin Formation from HMB Alone, Evidence for a Second Pathway? We found that solutions of one equivalent of trimethylbenzene and three equivalents of methanol or one equivalent of toluene and five equivalents of methanol yielded far more olefins (and alkanes) than one equivalent of HMB alone. HMB and several equivalents of water was not appreciably more reactive. Yet, HMB alone can be converted to a moderate yield of olefins using forcing conditions, either higher temperature (Figure 3c) or especially a higher acid site density (Figure 4d). In the 1961 study of the paring reaction, HMB (in a hydrogen stream) was hydrocracked to isoalkanes and lighter methylbenzenes (or their corresponding naphthenes) in good yields at 350 °C on a bifunctional nickel sulfide/silica−alumina catalyst. We recently reported that methylbenzenes trapped in the cages of HSAPO-34 slowly decompose to ethylene and propene after the cessation of methanol flow. In the present investigation, one can imagine HMB substituting for methanol as the methylating agent in Scheme 5. This might occur directly or through mediation of a hypothetical framework methoxonium species prepared as in Scheme 3. It is more difficult to use this idea to rationalize the elimination of olefins from methylbenzenes trapped in HSAPO-34 cages. Not even benzene can pass through the 0.38 nm windows connecting the cages of HSAPO-34 (which has the CHA topology). Furthermore, on active HSAPO-34 catalysts of the type studied in ref 11, only a few percent of the cages contained methylbenzene molecules, so these would appear to have been isolated. It may be that paring is more important on HSAPO-34 than on HBeta. But on HBeta, side-chain methylation is the preferred route with excess methanol, as originally proposed by Mole and co-workers for zeolite HZSM-5.

Conclusions

This investigation has provided the most detailed description yet of a hydrocarbon pool pathway for MTO catalysis on a solid acid catalyst. Side-chain methylation of hydrocarbon pool species leads to olefinic products. We observed isopropyl- and ethyl-substituted methylbenzenes in the product streams; while these species are probably closely related to intermediates in olefin synthesis, at least some of them also form by back-reaction of olefins and aromatics. Ethyl or isopropyl groups are more readily eliminated from aromatics in the presence of methanol, presumably after several ring methylation steps. Side-chain methylation conserves the carbon isotope distribution in the rings of hydrocarbon pool species, and the ring carbon scrambling seen here is accounted for by secondary reactions. Pentamethylbenzene was the major volatile product of HMB, and this was explained by a disproportionation reaction yielding the heptamethylbenzenium cation **3** as a species trapped in the zeolite. Equilibration of cation **3** with the exocyclic olefin **12** leads to H/D exchange for HMB on the zeolite.

Methylbenzenes alone do decompose on HBeta to form olefins, but to a lesser extent than with added methanol. The relationships between the average number of methyl groups on benzene rings and the activity and selectivity for olefin products that we previously reported on HSAPO-34 are supported by this investigation.

Acknowledgment. This work was supported by the National Science Foundation (CHE-9996109) and the U.S. Department of Energy (DOE) Office of Basic Energy Sciences (BES) (Grant No. DE-FG03-93ER14354). Alain Sassi acknowledges the Deutsche Forschungsgemeinschaft (DFG) for their financial support. Computer resources were provided by the National Energy Research Supercomputer Center (NERSC), Berkeley, CA.

References and Notes

(1) Chang, C. D. *Catal. Rev.* **1983**, *25*, 1−118.
(2) Stöcker, M. *Microporous Mesoporous Mater.* **1999**, *29*, 3−48.
(3) Keil, F. J. *Microporous Mesoporous Mater.* **1999**, *29*, 49−66.
(4) Chang, C. D. *Shape-selective catalysis: chemicals synthesis and hydrocarbon processing*; Song, C., Garces, J. M., Sugi, Y., Ed.; ACS Symposium Series 738, Washington, DC, 2000.
(5) Goguen, P. W.; Xu, T.; Barich, D. H.; Skloss, T. W.; Song, W.; Wang, Z.; Nicholas, J. B.; Haw, J. F. *J. Am. Chem. Soc.* **1998**, *120*, 2651−2652.
(6) Haw, J. F.; Nicholas, J. B.; Song, W.; Deng, F.; Wang, Z.; Heneghan, C. S. *J. Am. Chem. Soc.* **2000**, *122*, 4763−4775.
(7) Mikkelsen, O.; Ronning, P. O.; Kolboe, S. *Microporous Mesoporous Mater.* **2000**, *40*, 95−113.
(8) Dahl, I. M.; Kolboe, S. *J. Catal.* **1994**, *149*, 458−464.
(9) Dahl, I. M.; Kolboe, S. *J. Catal.* **1996**, *161*, 304−309
(10) Song, W.; Haw, J. F.; Nicholas, J. B.; Heneghan, K. *J. Am. Chem. Soc.* **2000**, *122*, 10726−10727.
(11) Song, W.; Fu, H.; Haw, J. F. *J. Am. Chem. Soc.* **2001**, *123*, 4749−4754.
(12) (a) Arstad, B.; Kolboe, S. *Catal. Lett.* **2001**, *71*, 209−212. (b) Arstad, B.; Kolboe, S. *J. Am. Chem. Soc.* **2001**, *123*, 8137−8138.
(13) Xu, T.; Barich, D. H.; Goguen, P. W.; Song, W.; Wang, Z.; Nicholas, J. B.; Haw, J. F. *J. Am. Chem. Soc.* **1998**, *120*, 4025−4026.
(14) NIST Chemistry WebBook (http://webbook.nist.gov/chemistry/).
(15) Sullivan, R. F.; Egan, C. J.; Langlois, G. E.; Sieg, R. P. *J. Am. Chem. Soc.* **1961**, *83*, 1156−1160.
(16) Mole, T.; Whiteside, J. A.; Seddon, D. *J. Catal.* **1983**, *82*, 261−266.

(17) Mole, T.; Bett, G.; Seddon, D. *J. Catal.* **1983**, *84*, 435−445.
(18) Song, W.; Nicholas, J. B.; Sassi, A.; Haw, J. F. *Catal. Lett.*, submitted.
(19) Murray, D. K.; Chang, J. W.; Haw, J. F. *J. Am. Chem. Soc.* **1993**, *115*, 4732−4741.
(20) Xiong, Y. S.; Rodewald, P. G.; Chang, C. D. *J. Am. Chem. Soc.* **1995**, *117*, 9427−9431.
(21) Nicholas, J. B.; Haw, J. F. *J. Am. Chem. Soc.* **1998**, *120*, 11804−11805.
(22) Doering, W. von E.; Saunders, M.; Boyton, H. G.; Earhart, H. W.; Wadley, E. F.; Edwards, W. R.; Laber, G. *Tetrahedron* **1958**, *4*, 178−185.
(23) Sefcik, M. D. *J. Am. Chem. Soc.* **1979**, *101*, 2164−2170.
(24) Ignatyev, I. S.; Sundius, T. *Chem. Phys. Lett.* **2000**, *326*, 101−108.